**Response to reviewer:** *Mekhaldi et al.: "Radionuclide wiggle-matching reveals a non-synchronous Early Holocene climate oscillation in Greenland and Western Europe around a grand solar minimum"*

**First, the authors would like to thank the reviewer for their positive and constructive comments. The manuscript was amended following their recommendations to the best of our ability. Herein is a point-by-point reply to the reviewer's comments.**

*In their manuscript, Mekhaldi et al. present a very interesting study comparing the palaeo-environmental records of the Greenland ice-cores and the varved Meerfelder Maar (MFM) in the early Holocene. Importantly, the authors are able to align the chronologies of the respective records using Beryllium-10 (10Be) concentration data from both archives, thus demonstrating that the "11.4 ka event" (Greenland) and "Preboreal Oscillation (PBO)" (MFM) were asynchronous and therefore not, as has been previously suspected, expressions of the same underlying climatic "event". The manuscript is well written, based on sound science, and the final discussion is balanced and well argued. I recommend that this manuscript be accepted for publication in Climate of the Past pending very minor revisions.*

Thank you.

*Scientific questions:*

*L21: I do not know the term "Superepoch" – is it widely used? (Excuse my ignorance! Google also didn't help…!)*

Here we use the term "Superepoch" in the light of the new formalization of the Holocene subdivision (Walker et al., 2019).

*L21: Can the term "climate events" be defined? (Perhaps not within the abstract, but below – perhaps ~L44). Would the term "oscillations" be more appropriate (in the Abstract, at least), which I think is less 'loaded' in terms of assumed prior synchroneity/a common ultimate trigger?)*

Climate "event" has been replaced with "oscillation" in the abstract. Furthermore, we believe that the use of "events" is implicitly specified in the first line of the introduction as "past climate changes", and in the first paragraph overall. An example (the PBO) is therein defined as representing a short-lived "a cold spell".

*L53: I do not understand "an event that spread over time"*

To clarify the meaning of the sentence, we replaced "an event that spread over time" with "an event that gradually propagated over time".

*L55: By "mechanisms", do you mean ultimate causes/triggers, or propagation mechanisms (or both)?*

We mean both and clarified this by adding "triggering and propagation mechanisms" to the sentence.

*L56-62: I would like a figure referred to here that displays what is being discussed (i.e. the common signals in 10Be and Delta14C through this period).*

We have added a panel with Delta14C covering this period in Fig. 1.

*L107-108: please could you expand a little further upon this methodology ("The synchronization of the different radionuclide records was computed following the methodology described by Adolphi and Muscheler (2016)").*

We have supplemented this section of the manuscript with: "This method employs the same Bayesian approach as used for wiggle-matching tree-ring $^{14}$C sequences to the radiocarbon calibration curve (Bronk Ramset et al. 2001, Radiocarbon). It exploits the fact that the spacing between samples is precisely known from varve- and layer-counts, and that hence, the probability density functions from individual samples can be combined using Bayes' theorem. In analogy to radiocarbon wiggle-matching of tree-rings, we use one record (for example $^{14}$C production rate) as our "calibration curve" while the other record serves as our "tree-rings" (e.g., MFM and GRIP $^{10}$Be). By shifting one relative to the other we can thus, estimate a probability density function of the timescale-difference between the two records. Further details can be found in Adolphi and Muscheler (2016) and Bronk Ramsey et al. (2001)."

*L128: could these 14C atmospheric production rate data (from Muscheler et al. 2014) not also be included on Fig. 1? I think that this would be useful (since these data are being discussed).*

See the addition of Delta14C in Fig. 1, as suggested by the reviewer in a comment above. In addition, the $^{14}$C production rate data is shown in Fig. 2 for which we have added a reference to in the text mentioned here.

*L131-133: But there is also a ~40 year trough in the MFM 10Be data that is not seen in the GRIP data, rendering the ~100 year chronological offset questionable. (I.e., the signal structure is different, making it difficult to suggest that the difference is JUST one of offset chronology.)*

It is true that some short-lived features in the radionuclide data (MFM and GRIP 10Be and 14C production rate) disagree with one another. However, we mostly make use of the overall longer-term and prominent increase in radionuclide production rate (caused by the grand solar minimum) for synchronizing these records. System effects inherent to such data will typically lead to such short-term discrepancies and this is also taken into account within the 20% uncertainty.

We have added to section 3.1 the following: "[…] although some short-term features are not visible in all records such as a 40-year long trough in the MFM 10Be data (ca. 11,290-11,250 years BP)."

*L162-164: although "difficult to quantify objectively", is there any covariance between any of the MFM palaeoenvironmental data and the 10Be signal (or its artefact, if primary agreement with Greenland 10Be deposition is assumed)? E.g., is there any environmental explanation for the previously noted decrease in 10Be at MFM ca. 11,290-11,250 cal BP that is not seen in the Greenland 10Be data? (N.B. the correlation matrix presented in Fig.5 is of relevance here.)*

The review could be correct that the trough at MFM ca. 11,290-250 cal BP may be explained by catchment/environmental effects (see Sup. Fig. 1). However, the overall structure caused by the grand solar minimum is consistent with GRIP 10Be and 14C production rate. In addition, we cannot correct for these small effects as the catchment proxies from MFM appears to be well-correlated with solar activity at the time (see correlation matrix in Fig. 5). Therefore, removing covariance between MFM 10Be and MFM catchment proxies would effectively remove the solar signal from the former.

*L167-168: If JUST wanting to compare between MFM and Greenland (i.e. the representation of their respective "PBO" and "11.4ka event"), is it not preferable to JUST compare the fluctuations of 10Be at the two sites directly (i.e. placing the MFM chronology on to GICC05 or vice versa)? For the purpose of assessing the synchrony/asynchrony of these climatic signals, the absolute ages are not important – you are JUST interested in the relative chronology of the two sites (MFM vs Greenland and, therefore, PBO vs 10.4ka event). Surely placing both (MFM and Greenland) separately on to IntCal creates additional unnecessary uncertainty for this purpose? (Though obviously placing on to IntCal allows for the comparison of other data too – e.g. tree-ring 14C.)*

*You discuss around this point above (L154-157), but opt for the modeling of both on to IntCal, rather than the direct comparison of MFM and Greenland. But wouldn't the subsequent discussion here be (even) more robust if you just used the MFM data on GICC05 (or Greenland on MFM chronology)?*

We agree with the reviewer's comment that placing both MFM and GICC05 chronologies separately on IntCal creates additional uncertainty, though small. However, we feel it is more important to provide the best possible absolute age for the events discussed. In addition and as also pointed out by the reviewer, providing an absolute age offers the non-negligible opportunity for future studies and data to be compared more directly and robustly. We thus believe synchronizing MFM and GICC05 to IntCal is more beneficial than only considering the relative chronology of the two sites.

*L205-208: it is probably fair to say that "When looking at the temperature proxy and varve thickness from MFM (Fig. 3d-e), we do not find any event that is coeval with the 11.4 ka event in Greenland". However, as you go on to note subsequently, "Ticlr data (Fig. 3e) gradually decreased from ca. 11,490 years BP only to be interrupted by a small increase around 11,300 years BP. The low Ticlr data suggest less runoff probably related to drier conditions". The structure of this Ticlr data looks visually similar to that of the Greenland accumulation anomalies (which are limited to a subset of the time range covered by the other proxies). Could it not be that this is showing some commonality in (climatic) driver, even though the isotopic signals (representing an alternative climatic variable, or subtly different combination of climatic/environmental variables) are not showing commonality through this period?*

We thank the reviewer for rightfully pointing out that the structure of the Ti(clr) data looks similar to the Greenland accumulation anomalies – a point that was perhaps not stated clearly enough. Although we want to remain cautious about over-interpreting the proxy data, we have added to the manuscript: "The low Ti$_{clr}$ data suggest less runoff probably related to drier conditions [*which shows some commonality with the conditions in Greenland at that time (11.4 oscillation) evidenced by the lower accumulation rate.*]"

*L214: it might be useful to define "grand solar minimum" for a more generalist audience (here, or at some other suitable place in the text)*

In the second paragraph of the introduction (L56), we now specify: *"grand solar minimum (persistently low solar activity resulting in significantly higher radionuclide production rate)".*

*L333: state when/how long the Maunder Minimum was (again for the more generalist audience)?*

We complemented the mention of the Maunder minimum with its date "(1645-1715 Common Era)".

*Fig.1: why are your new data presented with error bars, but not the previously published (Czymzik et al. MFM and Adolphi et al. Greenland) data?*

We plotted error bars for all data.

*Figure 5: would it be clearer to only give half the correlation matrix (since the upper left portion is the same as the lower right portion)?*

We appreciate the review's concern for clarity of Fig. 5 but we do believe the figure is clearer as a square. For instance, if the reader wants to know the correlation between GRIP 10Be and all other data, they can simply follow its entire row or column. This would not be possible if the upper left or lower right portion is removed.

Language suggestions:

**The authors take the opportunity here to thank the reviewer for contributing to enhance the quality of the language in the manuscript.**

*LL52, 130, 249: change "chronology" to "chronological"*

Changed.

*L116 & 118: delete "with"*

Deleted.

*L135: change to "timescale" (singular)*

Changed.

*L169: change to "climatic proxy data"*

Changed.

*L183: delete "of"*

Deleted.

*L202: delete "this means that"*

Deleted.

*L205: insert "…varve thickness [data]…"*

Inserted.

*L261: delete "to"*

Already deleted.

*L265: change "sun" to "solar"*

Here, we would like to hold on to the use of "Sun-climate link" as it is a commonly used phrase when discussing solar forcing on climate.

*L285: by "boundaries" do you mean "boundary conditions"?*

We do, and added "climate boundary conditions".

*L307: change "is" to "are"*

Changed.

*L342: change "of which" to "to which" (and delete subsequent "to")*

Changed/deleted.

*L352: change to "routinely released"*

Changed.

*L354: change "detangle" to "disentangle"*

Already changed.

Additional changes:

- Reference to Bronk Ramsey et al., Radiocarbon 2001 was added.

- Error bars of MFM 10Be data (red curve in Fig. 1) were fixed.

- The 10Be data from GRIP was erroneously referred to as "10Be concentration" on a few occasions when in fact we used "10Be flux". This has been corrected (see eg. L 100 in Marked Up manuscript).

# Radionuclide wiggle-matching reveals a non-synchronous Early Holocene climate oscillation in Greenland and Western Europe around a grand solar minimum

Florian Mekhaldi[1], Markus Czymzik[2], Florian Adolphi[1,3], Jesper Sjolte[1], Svante Björck[1], Ala Aldahan[4], Achim Brauer[5], Celia Martin-Puertas[6], Göran Possnert[7], and Raimund Muscheler[1]

[1]Department of Geology - Quaternary Sciences, Lund University, 22362 Lund, Sweden
[2]Leibniz-Institute for Baltic Sea Research Warnemünde (IOW), Marine Geology, 18119 Rostock, Germany
[3]Physics Institute, Climate and Environmental Physics & Oeschger Centre for Climate Change Research, University of Bern, 3012 Bern, Switzerland
[4]Department of Geology, United Arab Emirates University, 15551 Al Ain, UAE
[5]GFZ-German Research Centre for Geosciences, Climate Dynamics and Landscape Evolution, 14473 Potsdam, Germany
[6]Department of Geography, Royal Holloway University of London, Egham, Surrey TW20 0EX, UK
[7]Tandem Laboratory, Uppsala University, 75120 Uppsala, Sweden

*Correspondence to*: Florian Mekhaldi (florian.mekhaldi@geol.lu.se)

**Abstract.** Several climate oscillations have been reported from the Early Holocene superepoch, the best known of these being the Preboreal oscillation (PBO). It is still unclear how the PBO and the number of climate oscillations observed in Greenland ice cores and European terrestrial records are related to one another. This is mainly due to uncertainties in the chronologies of the records. Here, we present new high resolution $^{10}$Be concentration data from the varved Meerfelder Maar sediment record in Germany, spanning the period 11,310-11,000 years BP. These new data allow us to synchronize this well-studied record as well as Greenland ice-core records to the IntCal13 time-scale via radionuclide wiggle-matching. In doing so, we show that the climate oscillations identified in Greenland and Europe between 11,450 and 11,000 years BP were not synchronous but terminated and began, respectively, with the onset of a grand solar minimum. A similar spatial anomaly pattern is found in a number of modeling studies on solar forcing of climate in the North Atlantic region. We further postulate that freshwater delivery to the North Atlantic would have had the potential to amplify solar forcing through a slowdown of the Atlantic meridional overturning circulation (AMOC) reinforcing surface air temperature anomalies in the region.

## 1 Introduction

One of the great challenges in paleoclimatology today is to better assess the spatial and temporal dynamics of past climate changes. This can only be achieved through robust and consistent chronologies for different records and different regions. Unfortunately, this is a challenging task and we often assume synchrony of such events by climate-tuning different records. One such example is the Preboreal oscillation (PBO) (Björck et al., 1996) and represents a cold spell which occurred shortly after the Younger-Dryas/Holocene transition. Indications of a cold phase have also been reported in a number of European terrestrial records, most of which use biological proxy and isotope data (Björck et al., 1996; Björck et al., 1997; Bos et al., 2007; Magny et al., 2007, van der Plicht et al., 2004; von Grafenstein et al., 1999). A cold and dry climate oscillation, thought to be related to the European PBO, has also been observed in the $\delta^{18}O$ and accumulation signals of a number of Greenland ice cores between 11,520-11,400 years before AD 2000 (b2k) and referred to as the 11.4 ka event (Rasmussen et al., 2007; 2014). Due to chronological uncertainties, it is however unclear whether the 11.4 ka event in Greenland and the European PBO represent one single and synchronous widespread event, an event that gradually propagated over time, or whether the European PBO is unrelated to the 11.4 ka event in Greenland. These open questions limit our understanding of the underlying triggering and propagation mechanisms of these climate changes.

Around this period, one of the largest and longest-lasting grand solar minimum (persistently low solar activity resulting in significantly higher radionuclide production rate) of the Holocene occurred between 11,280-10,960 years before AD 1950 (BP). This was evidenced by beryllium-10 ($^{10}$Be) data in the GISP2 and GRIP ice cores in central Greenland (Finkel and Nishiizumi, 1997; Muscheler et al., 2004; Adolphi et al., 2014) and by $\Delta^{14}C$ ($^{14}C/^{12}C$ corrected for fractionation and decay, relative to a standard, and noted as $\Delta$ in Stuiver and Polach (1977)) derived from tree rings (Reimer et al., 2013). This substantial change in solar activity (from high to persistently low) offers an advantage to us for synchronizing time-scales as it has left a clear imprint on the atmospheric production rate of the cosmogenic radionuclides $^{10}$Be and $^{14}$C (Fig. 1). That is, these radionuclides are produced by a nuclear cascade that is triggered when cosmic rays enter the atmosphere. The Earth is shielded, to some extent, from these cosmic rays by the fluctuating strength of the helio- and geomagnetic fields. Therefore, radionuclides carry in part the signal of solar activity, which is then stored in natural archives such as in polar ice caps or lake sediments ($^{10}$Be) as well as in tree rings ($^{14}$C). In consequence, we can use these global fluctuations in atmospheric production rate of radionuclides to synchronize records from different environmental archives and investigate the timing of climate events during the earliest part of the Holocene (Southon, 2002; Muscheler et al., 2014; Adolphi and Muscheler, 2016).

Here we present new high-resolution $^{10}$Be concentration measurements from the well-studied varved Meerfelder Maar sediment record (MFM) in western Germany, spanning across these large fluctuations in solar activity from 11,310 to 11,000 years BP. Because of its limited catchment area and the existence of $^{10}$Be data covering the Late Glacial-Holocene transition (Czymzik et al., 2016), MFM represents an ideal location for the aim of this study. As such, the new $^{10}$Be data allow us to synchronize MFM and Greenland ice core records with the IntCal13 time-scale through wiggle-matching of these different radionuclide records. We can then investigate the timing of the fluctuations observed in the corresponding paleoclimate records at a high chronological precision and assess their relationship in regard to changes in solar activity.

## 2 Methods

### 2.1 Preparation of sediment [10]Be samples

The new [10]Be samples come from the composite sediment profile MFM09 (Martin-Puertas et al., 2012a) which was retrieved at MFM, a deep crater lake situated in the Eiffel region in western Germany that is annually laminated (varved) throughout most of the Holocene (Brauer et al., 2000). About 0.25 g of dried and crushed material was taken for each sample with a temporal resolution of 3 and 10 years (see dataset) and 0.5 mg of [9]Be carrier was added. [10]Be was extracted from the sediment samples at the [10]Be laboratory of the Earth Sciences Department of Uppsala University, Sweden, following the methodology described by Berggren et al. (2010). All samples were measured using the Accelerator Mass Spectrometer (AMS) of the Tandem laboratory in Uppsala. The [10]Be concentration (in atoms/g) of each sample is calculated based on the [10]Be counts $R$ to [9]Be counts $Rst$ ratio and taking in consideration the NIST SRM 4325 reference standard ([10]Be/[9]Be = 2.68 10^{-11}), the weights of the carrier $W_C$ and of the sample $W_S$ as well as the Avogadro constant $N_A$ and atomic weight $A_r$ of beryllium:

$$^{10}Be\ conc. = \frac{R}{R_{st}} * 2.68\ 10^{-11} * \frac{W_C}{W_S} * \frac{N_A}{A_r}$$

### 2.2 Chronologies and synchronization

The paleoclimate data investigated henceforth come from different studies, with different records and thus different chronologies. The new sediment [10]Be concentration data come from MFM, the chronology of which (MFM2012) was established using mainly microscopic varve counting fixed on an absolute time-scale via tephrochronology as well as radiocarbon dating with a maximum varve counting error of up to 110 years (Brauer et al., 2000; Martin-Puertas et al., 2012a). A more recent chronology (MFM2015) exists which includes the identification and age of the Vedde Ash although it remains unchanged for the Holocene part (Lane et al., 2015), which is the period of focus in this study. We also use published [10]Be flux data (Adolphi et al., 2014) from the GRIP ice core in central Greenland and within the Greenland Ice Core Chronology (GICC05) framework (Rasmussen et al., 2006; Vinther et al., 2006; Svensson et al., 2008; Seierstad et al., 2014). Finally, we use ^{14}C production rate data (Muscheler et al., 2014) inferred from the IntCal13 ^{14}C calibration curve (Reimer et al., 2013) as the anchoring record for our synchronization. That is, we synchronize the MFM2012 time-scale (using our [10]Be concentration data) as well as the GICC05 time-scale (using the GRIP [10]Be flux data) to IntCal13 (using the ^{14}C production rate data).

The synchronization of the different radionuclide records was computed following the methodology described in Adolphi and Muscheler (2016). This method employs the same Bayesian approach as used for wiggle-matching tree-ring ^{14}C sequences to the radiocarbon calibration curve (Bronk Ramsey et al., 2001). It exploits the fact that the spacing between samples is precisely known from varve- and layer-counts, and that hence, the probability density functions from individual samples can be combined using Bayes' theorem. In analogy to radiocarbon wiggle-matching of tree-rings, we use one record (for example ^{14}C production rate) as our "calibration curve" while the other record serves as our "tree-rings" (e.g., MFM and GRIP [10]Be). By shifting one relative to the other we can thus, estimate a probability density function of the timescale-difference between the two records. Further details can be found in Adolphi and Muscheler (2016) and Bronk Ramsey et al. (2001).

116 For these calculations we linearly detrend all radionuclide records between 11,000 and 11,800 years BP and

117 assumed a production rate uncertainty of 20% for all records, which corresponds to the root mean square error

118 between the records after synchronization.

119

120 **3 Results**

121 **3. 1 Meerfelder Maar $^{10}$Be concentrations**

122 The new $^{10}$Be concentration measurements from MFM are displayed in Fig. 1, alongside $^{10}$Be flux data from the

123 GRIP ice core in central Greenland (Finkel and Nishiizumi, 1997; Muscheler et al., 2004; Adolphi et al., 2014),

124 and older $^{10}$Be concentration data from MFM for the Late Glacial-Holocene transition (Czymzik et al., 2016).

125 Each dataset is plotted on its original time-scale – that is, the MFM2012 chronology (Brauer et al., 2000; Martin-

126 Puertas et al., 2012a) and the GICC05 chronology (Rasmussen et al., 2006; Vinther et al., 2006; Svensson et al.,

127 2008; Seierstad et al., 2014). The most striking feature of these datasets is the approximately 250-year long

128 period of increased $^{10}$Be concentration around 11,150 years BP. The most likely explanation for this increase is a

129 decrease in the intensity of the heliomagnetic field (solar activity) leading to an increased impingement of Earth

130 by galactic cosmic rays and thus, an increased atmospheric production rate of $^{10}$Be and $^{14}$C nuclides. It was also

131 shown that meteorological and catchment influences on $^{10}$Be deposition are likely small at MFM (Czymzik et al.,

132 2016). The high resolution of our $^{10}$Be measurements allows us to observe finer structures within this period of

133 increased $^{10}$Be concentration. One example is the double peak structure at 11,040 and 11,200 years BP, which is

134 also present in $^{14}$C atmospheric production rate data (Muscheler et al., 2014; Fig. 2), but not well-expressed in

135 the GRIP $^{10}$Be data. Finally, it is of importance to note that although the increased production around 11,150

136 years BP is observed in all these radionuclide records, there is an apparent chronological offset at its onset

137 around 11,300 years BP (Fig. 1). More specifically, the $^{10}$Be flux data from GRIP begin to increase around

138 11,320 years BP whereas a similar increase is seen in the $^{10}$Be concentration from MFM about a hundred years

139 later although some short-term features are not visible in all records such as a 40-year long trough in the MFM

140 $^{10}$Be data (ca. 11,290-11,250 years BP).

141

142 **3. 2 Time-scale synchronization**

143 The Greenland ice core time-scale is characterized by an accumulating layer counting uncertainty back in time

144 (Rasmussen et al., 2006) as are chronologies based on sediment varve counting such as MFM. In comparison

145 tree ring chronologies, underlying the $^{14}$C calibration record, are considered accurate with virtually no dating

146 uncertainty for the Holocene period (Reimer et al., 2013). Considering the different time-scale uncertainties, it is

147 challenging to compare the timing of short-lived climate oscillations such as the PBO/11.4 ka event. Here we use

148 the global signature common to all cosmogenic radionuclide records as a synchronization tool (Muscheler et al.,

149 2008; 2014). More specifically, we use the large fluctuations in both the MFM and GRIP $^{10}$Be data to

150 synchronize these records onto the chronologically more accurate and precise IntCal13 time-scale (Czymzik et

151 al., 2018). It was previously shown that GICC05 increasingly overestimates age during the Holocene, compared

152 to IntCal13 (Muscheler et al., 2014) and this time-scale difference is estimated to increase to 67 ($\pm$ 6) years at

153 11,000 years BP (Adolphi and Muscheler, 2016). We use the same Bayesian wiggle-matching approach as in

154      Adolphi and Muscheler (2016), but here for the period 11,000-11,800 years BP to synchronize both the MFM

155      sediment and Greenland ice core records onto IntCal13.

156          Figure 2 shows both the ice-core and sediment-core $^{10}$Be data once synchronized onto the IntCal13

157      time-scale using the $^{14}$C production rate from Muscheler et al. (2014), with the corresponding probability density

158      functions displayed on the right-hand panel. We find that the MFM $^{10}$Be data fit best with $^{14}$C by adding 20 years

159      to MFM2012 (+6/-19 years uncertainty with a 95.4% confidence interval), whereas the GRIP $^{10}$Be data fit best

160      with $^{14}$C by shifting GICC05 78 years towards present (+32/-8 years uncertainty with a 95.4% likelihood

161      interval). When comparing GICC05 directly to MFM2012, we find that the best fit occurs by shifting GICC05

162      72 years towards MFM2012 (+4/-8 years with a 95.4% likelihood interval). There is thus a difference of 26

163      years (72 +4/-8 years vs. 98 +33/-21 years) when comparing GICC05 and MFM2012 directly, rather than

164      synchronizing them to IntCal13 first which illustrates the uncertainties inherent to this exercise. In the following,

165      we will compare GICC05 and MFM2012 when synchronized to IntCal13 as it is the more robust time-scale and

166      thus consider the combined chronology offset of 98 (+33/-21) years. Another uncertainty from these estimates

167      arises from the influence of climate on the cosmogenic signal of all radionuclides (Adolphi et al., 2014;

168      Muscheler et al., 2008; Pedro et al., 2012). For instance, $^{14}$C oxidizes to form $^{14}$CO$_2$ and enters the carbon cycle

169      while $^{10}$Be readily attaches to aerosols and is thus influenced by precipitation. Even though $^{10}$Be deposition is not

170      expected to have strong environmental influences at MFM (Czymzik et al., 2016), this was taken into account

171      within the 20% uncertainty since these effects are difficult to quantify objectively.

172

173      **3.3 Anomalies in paleoclimate proxies between 11,450-11,000 years BP**

174      If we correct the GICC05 and MFM2012 timescales for their respective offsets to IntCal13, we can compare

175      Early Holocene climate in Greenland to data from MFM with a high chronological precision. Figure 3 displays a

176      selection of climatic proxy data from both Greenland ice cores and the varved MFM record on the IntCal13

177      time-scale, as per Fig. 2. In addition, both $^{14}$C atmospheric production rate and GRIP $^{10}$Be flux data are shown as

178      a general indicator of changes in solar activity (Fig. 3a). The stack of $\delta^{18}$O anomalies from four Greenland ice

179      cores (DYE-3, GRIP, NGRIP, and Renland - Fig. 3b) can be related to surface air temperature around Greenland

180      (Rasmussen et al., 2007; Vinther et al., 2009) and shows one negative fluctuation between 11,400-11.250 years

181      BP. Following this oscillation, the Greenland $\delta^{18}$O anomaly record remains largely constant and positive. In

182      addition, we also use the accumulation rate anomaly stack (Fig. 3c) from the DYE-3, GRIP, and NGRIP ice

183      cores (Rasmussen et al., 2007) to illustrate changes in snow accumulation rates over Greenland. Here again, a

184      negative fluctuation is observed between 11,400-11.250 years BP. Then, we make use of the MFM $\delta$D records

185      of n-alkanes (Fig. 3d) that has been interpreted as a proxy for precipitation $\delta$D (Rach et al., 2014) which,

186      similarly to $\delta^{18}$O in Greenland, can thus be regarded as indicative of distance from, and temperature/humidity at

187      the moisture source (Dansgaard, 1964) as well as fractionation related to air temperature. As opposed to the

188      Greenland stack, the $\delta$D data show no fluctuations between 11,400-11,250 years BP with $\delta$D$_{aq}$ remaining

189      constant and $\delta$D$_{terr}$ showing an increasing trend. Then at 11,250 years BP, both $\delta$D series depict a 20% drop that

190      persists until 11,100 years BP. To test the spatial scale to which the $\delta$D record from MFM can be representative,

191      we have investigated the spatial relationship between surface air temperature (SAT) in the NOAA-CIRES 20th

192      climate reanalysis V2c (20CR; Compo et al., 2011) and $\delta$D in precipitation from the Trier meteorological station

(about 50 km SW of MFM). It can be seen from Fig. 4 that there is a significant relationship (p <0.1) between annual precipitation δD from the Trier station (IAEA/WMO, 2006) and annual SAT over most of western Europe. In addition, Fig. 4 also points to a relationship between annual SATs over Greenland-Iceland and annual $\delta^{18}O$ at Summit (Steig et al., 1994; White et al., 2009). Finally, we also show varve thickness changes at MFM that were primarily controlled by runoff from the catchment. After a period of low varve thickness, a sharp increase occurred 11,250 years BP followed by a gradual decrease and a second but very small increase around 11,080 years BP. Titanium centered-log ratio data ($Ti_{clr}$), determined by micro X-ray fluorescence (μ-XRF) from the same MFM sediment composite profile (Martin-Puertas et al., 2017), confirm the interpretation that the variance in varve thickness at the time was mostly controlled by detrital supply to the lake (Fig. 3e). It is important to mention that on a longer time perspective, the changes described above in the sediments of MFM (Martin-Puertas et al., 2017; Rach et al., 2012) do not exceed other fluctuations in varve thickness and $Ti_{clr}$.

## 4 Discussion

### 4.1 Timing and interpretation of anomalies between 11,450-11,000 years BP

In Greenland, a cold and dry climate episode occurred around 11,400-11,250 years BP known as the 11.4 ka event (Rasmussen et al., 2007). This is evidenced by a significant drop in the signal of the Greenland ice core $\delta^{18}O$ stack as well as in the accumulation stack (Fig. 3b-c). By shifting GICC05 78 years towards present, the central part of the 11.4 ka event (lowest value in $\delta^{18}O$) is dated to about 11,372-11,272 (+32/-8) years BP which is consistent with GICC05 within the combined uncertainty of our synchronization and the maximum counting error in GICC05. When looking at the temperature proxy and varve thickness data from MFM (Fig. 3d-e), we do not find any event that is coeval with the 11.4 ka event in Greenland. Interestingly though, $Ti_{clr}$ data (Fig. 3e) gradually decreased from ca. 11,490 years BP only to be interrupted by a small increase around 11,300 years BP. The low $Ti_{clr}$ data suggest less runoff probably related to drier conditions which shows some commonality with the conditions in Greenland at that time (11.4 oscillation) evidenced by the lower accumulation rate. Therefore, a possible link to the dry "Rammelbeek Phase" described from the Borchert peat sequence in the Netherlands (van der Plicht et al., 2004; Bos et al., 2007) may be tentatively put forward although chronological uncertainties hinder proving this. We can now also confidently deduce that the termination of the $\delta^{18}O$ and accumulation anomalies in Greenland (the 11.4 ka event) is synchronous with a large decrease in solar activity (Fig. 3a-c). More specifically, high levels of solar activity prevailed throughout the occurrence of the 11.4 ka event in Greenland. Then as solar activity started to decrease (circa 11,250 years BP) into a grand solar minimum that lasted for about 250 years, climate in Greenland switched back to warmer and wetter conditions with higher $\delta^{18}O$ values and accumulation rate. This is in accordance with the suggestion of an abrupt warming (4° ±1.5°) in Greenland following the event, based on $\delta^{15}N$ in the GIPS2 ice core (Kobashi et al., 2008). The rapid transition towards positive accumulation anomalies occurred over a few decades only.

While climate over Greenland following the 11.4 ka event returned rapidly to warmer and wetter conditions, all proxies from MFM sediments (Fig. 3d-e) show fluctuations around 11,250 years BP (henceforth MFM oscillation). In particular, aquatic δD data from small-chain alkanes (Rach et al., 2014) show a clear oscillation with a 20% drop around 11,250 years BP (Fig. 3d) while terrestrial δD data show a decrease reaching

levels seen about 11,500 years BP. This deuterium depletion in the alkanes most likely mirrors a depletion of deuterium in precipitation which can be explained, in part, by lower air temperatures over western Europe in view of Fig. 4. Simultaneously, varve thickness and $Ti_{clr}$ show a rapid increase at 11,250 years BP (Fig. 3e) denoting a likely increasing detrital contribution to this varve thickening. When considered into a longer time perspective (Martin-Puertas et al., 2017), this varve increase reaches the level of other fluctuations that are unrelated to known Early Holocene oscillations in North-Atlantic climate. Nevertheless, this shift at 11,250 year BP does correspond to a change in the composition of the sediments as Martin-Puertas et al. (2017) defined a compositional boundary of MFM varves at 11,230 years BP (11,250 years BP on the IntCal13 time-scale), based on μ-XRF scanning analyzed with Ward's clustering methods. By synchronizing MFM2012 onto IntCal13 (Fig. 2), we find that this compositional boundary is also coeval with the onset of the grand solar minimum (Fig. 3) although the cause of this change is difficult to assess. In fact, $Ti_{clr}$ as well as ln(Si/Ti) and ln(Ca/Ti), generally regarded by Martin-Puertas et al. (2017) as indicating relative changes of biogenic silica concentrations and authigenic calcite precipitation, are significantly correlated to the new [10]Be concentration measurements, but also to the GRIP [10]Be data and to ^{14}C atmospheric production rate (Fig. 5 and Sup. Fig. 1). Because GRIP [10]Be data and ^{14}C atmospheric production rate are unaffected by environmental changes at MFM, we suggest that the catchment area of MFM was likely influenced by the substantial changes in solar activity that characterized this period rather than [10]Be concentration at MFM being affected by this sediment compositional change. In support to this assumption, Czymzik et al. (2016) also reported negligible climate influences on [10]Be deposition at MFM, even across distinct climatological boundaries. It can also be seen that the second and smaller increase in varve thickness and $Ti_{clr}$ is coeval with a second dip in solar activity shortly after 11,100 years BP (Fig. 3a and 3e). Finally, it is worthwhile to note that the percentage values of *Pinus* pollen, biogenic silica, as well as pollen concentrations in MFM all decreased at 11,230-11,250 years BP while percentage values of *Betula* increased (Brauer et al., 1999). Although not interpreted by the authors, these changes echo the findings of Björck et al. (1997) who defined the PBO in terrestrial records of Sweden with a similar decrease of pollen concentrations and more notably of *Pinus* pollen percentages, interpreted as a set-back of tree vegetation in Southern Sweden. It should be stressed here that we cannot directly compare the palynology of MFM to these Swedish lakes because of the challenging interpretation of the former record as well as the chronological uncertainties and vicinity to the retreating Fennoscandian Ice Sheet of the latter records.

In summary, the radionuclide-based synchronization of the GICC05 and MFM2012 time-scales indicate a combined timing offset of up to 98 (+33/-21) years during the earliest part of the Holocene. Correcting for this offset, we observe that cold oscillations at both locations and inferred from water isotopes did not occur simultaneously between 11,450 and 11,000 years BP. We further note that this pattern appears to be coupled with large changes in solar activity, which leads us to suggest a causal link. More specifically, the cold and dry climate oscillation in Greenland (the 11.4 ka event) occurred under a period of high solar activity between c. 11,370-11,270 years BP, but did not leave a discernable imprint in either varve thickness or biomarker δD from MFM. Subsequently, solar activity dropped to a grand minimum that lasted for as long as 250 years. This change was coeval with the termination of the 11.4 ka event (Greenland) and the onset of the MFM oscillation with colder conditions inferred from δD data (Figs. 3d and 4). The ostensible link with solar activity which we infer in view of Fig. 3 resembles what has been described substantially in the recent literature and is discussed in the following section.

**4. 2 Solar forcing during 11,450-11,000 years BP**

Our suggestion of a causal Sun-climate link during the earliest part of the Holocene can be further supported by the spatial patterns of the 11.4 ka event in Greenland followed by a cold period at MFM starting at 11,250 years BP (MFM oscillation). Based on our synchronization of the different paleoclimate records, we find an asynchronous relationship between Greenlandic and European climate, characterized by cold and dry conditions over Greenland, but with no evidence of it at MFM, under high solar activity and a warm and wetter Greenlandic climate as well as a colder conditions at MFM for low solar activity (Fig. 3).

This pattern is consistent with a number of, but not all, climate modeling studies that find a top-down influence of solar activity on North Atlantic/European atmospheric circulation patterns. This forcing mechanism involves the increase in UV radiation during solar maxima years (Haigh et al., 2010; Lockwood et al., 2010) which enhances the production of stratospheric ozone and leads to stratospheric heating through increased absorption of long wave radiation (Haigh et al., 2010) especially at the equator. This increases the stratospheric temperature gradient between the equator and poles (Simpson et al., 2009) leading to an acceleration of the polar night jet (Kodera et al., 2002), which eventually propagates down to the troposphere via wave refraction (Matthes et al., 2006; Ineson et al., 2011). In turn, this leads to patterns in surface pressure and temperature which mimic those of the positive phase of the North Atlantic Oscillation in winter (Woollings et al., 2010; Ineson et al., 2011). The opposite mode applies during periods of solar minima. It should however be stressed that there is no consistent correlation between the NAO and solar forcing for the past centuries (Gray et al., 2013; Ortega et al., 2015) although a solar influence on the region is not necessarily related to the NAO (Moffa-Sánchez et al., 2014; Sjolte et al., 2018). Even though the spatial pattern we observe agrees well with a top-down solar forcing, other mechanisms cannot be excluded to lie behind the different North-Atlantic response patterns. Overall, it has to be kept in mind that different time periods with different climate boundary conditions could lead to shifting atmospheric patterns.

In the following we explore the solar hypothesis further by investigating a modern analogue with climate reanalysis data. Figure 6a shows the surface air temperature (SAT) anomalies in the North Atlantic region for periods of solar maxima compared to periods of solar minima in 20CR (mean ±1σ of the sunspot group numbers from Svalgaard and Schatten (2016) between 1946-2011, see Sup. Fig. 2). It can be seen from the SAT anomalies that a distinct antiphase pattern between Greenland and Europe is coincident with highs and lows in solar activity. That is, Greenland experiences lower SATs during winters of solar maxima compared to winters of solar minima whereas lower SATs are observed across Europe for winters of solar minima compared to winters of solar maxima. This highlights the correspondence between the solar influence on North-Atlantic climate which has been proposed to act during the 20th century and the synchronized climate proxy records during the Early Holocene, in terms of spatial distribution of SAT anomalies. Furthermore, this correspondence can also be qualitatively described by comparing the mean annual temperature anomalies at both Summit (central Greenland) and MFM (Fig. 6c-d) throughout an average of all 11-year solar cycles of the 20th century (Fig. 6b). Decadal temperature changes in 20CR at both Summit (blue curve in Fig. 6c) and MFM (red curve in Fig. 6d) agree qualitatively well with centennial $\delta^{18}O$ and $\delta D$ changes observed in Greenland ice cores and in MFM sediments and during the period ranging from 11,450 to 11,000 years BP (black curves in Fig.6c-d, note

the different time-axes). Of specific interest here is the average transition from high to low solar activity that is coincident with an annual temperature rise/drop of ca. 1K at Summit/MFM. Assuming changes in water isotopes to be, in part, indicative of regional temperature changes (Dansgaard, 1964; Masson-Delmotte et al., 2005; Rach et al., 2014; Fig. 4), this decadal pattern between Summit and MFM in climate reanalysis data mimics the centennial-scale climate changes that prevailed in Greenland and Europe throughout 11,450-11,000 years BP. Water isotopes are often dominated by a particular seasonal signal. It is therefore of interest to note that the spatial patterns observed in climate reanalysis are also present during the summer, although to a lesser degree (Sup. Fig. 3).

It should be noted that the efficiency of the top-down mechanism remains largely unexplored for centennial time-scales. For instance, previous studies have proposed a top-down solar influence on atmospheric circulation on similar time-scales for both Greenland (Adolphi et al., 2014) and MFM (Martin-Puertas et al., 2012b) leading to a similar spatial pattern in reanalysis data. The modeling results in these studies do however only investigate the effect of decadal (11-years) changes in solar activity. In contrast, it was also shown more recently that the centennial response of North-Atlantic atmospheric circulation to solar forcing is correlated to the second mode of atmospheric circulation, the Eastern Atlantic Pattern, rather than to the first mode, the NAO (Sjolte et al., 2018). The latter study consequently does not find a similar pattern in SAT anomalies between Greenland and western Europe.

For the same reasons, another uncertainty arises from the relevance of using 20th century climate reanalysis as an analogy of Early Holocene conditions. In particular, the Laurentide ice sheet (LIS) is known to have played an important role in the position of the North Atlantic eddy-driven jet by accelerating and displacing it southward (Merz et al., 2015). However, it is also known that the LIS waned to the point of separation with the Cordilleran at about 14,000 years BP (Dyke, 2004). According to a study based on a transient climate simulation from the LGM (Löfverström and Lora, 2017), this separation led to a shift in the dominant topographic stationary wave source in North America. This, in turn, induced a transition from a strong and subtropical jet stream to a weaker and more meridionally tilted jet stream and storm track, as observed for present conditions. This suggests that similar atmospheric processes could have been at play during the earliest part of the Holocene, relative to today, in spite of different boundary conditions. Furthermore, the results from Fig. 6 arise from an 11-year solar cycle forcing which is considerably weaker and less persistent than the potential solar forcing that the 11,400 years BP solar maximum to 11,200 years BP grand solar minimum could have provoked, leading to possibly different reactions due to feedback processes. In fact, both the $^{14}$C data and GRIP $^{10}$Be data shown in Fig. 2 depict one of the most prominent increases of the Holocene record (Vonmoos et al., 2006), in terms of both amplitude and duration of the grand solar minimum. In comparison, its duration represents twice the length of the longest grand minimum known from sunspot observations (Svalgaard and Schatten, 2016) and called the Maunder minimum (1645-1715 Common Era).

## 4.3 Solar-ocean coupling

The PBO has also been associated with an increase in freshwater supply hampering the Atlantic meridional overturning circulation (AMOC), possibly from the Baltic Ice Lake drainage and the rapidly waning Fennoscandian ice sheet (Björck et al., 1996; Hald and Hagen, 1998). It was next proposed by Fisher et al.

349 (2002) that an outburst of Lake Agassiz could represent the trigger of the PBO through an increased thickness
350 and extent of Arctic Ocean sea-ice pack. This would have resulted in an increased albedo as well as a slowdown
351 of North Atlantic Deep Waters (NADW) formation due to increased freshwater delivery to the North Atlantic.
352 However, the timing of the outburst event to which they attribute the PBO (11,335 cal yr BP) has rather large
353 uncertainties (± 130 to 230 years) due to the $\Delta^{14}C$ age plateau at this period. More recently, it was suggested that
354 even small changes in the prevalence of the AMOC can influence atmospheric circulation with couplings to the
355 NAO with an intensification of the former resulting in a negative index of the latter (Frankignoul et al., 2013).

356 To further investigate the potential spatial distribution of SAT anomalies due to a slowdown of the
357 AMOC, we again investigate 20CR for winters with a negative reconstructed AMOC index (Duchez et al., 2014)
358 compared to winters with a positive reconstructed AMOC index for the period 1961-2005 (Fig. 7a).
359 Interestingly, similar SAT anomalies subside as those for solar forcing. That is, an amplified meridional
360 temperature gradient with a colder Greenland and warmer western Europe are favoured in winters where the
361 AMOC is weaker, relative to winters where it is stronger. Although it is difficult to obtain direct evidence of an
362 AMOC slowdown during the Early Holocene, it is conceivable that the waning Fennoscandian ice sheet would
363 have routinely released enough freshwater to weaken and condition the AMOC for the onset of the 11.4 ka event
364 in Greenland. This result could also be explained by the influence of the NAO on the AMOC index, as it is
365 difficult to disentangle these tightly coupled processes (McCarthy et al., 2015). In this case, the persistent high
366 levels of solar activity, which also can favor such temperature and pressure patterns, could represent a potential
367 trigger for these climate oscillations. Figure 7b depicts the large temperature differences for winters where both
368 high solar activity and a weak AMOC prevailed during the period 1961-2005, with up to a -4K anomaly in
369 western Greenland. This however needs to be treated with caution due to the relatively short period of
370 observation that results in very few years where such solar activity and AMOC conditions existed in parallel
371 (Sup. Fig. 4).

372 In addition, a coupling between solar and freshwater forcing could also explain the lack of significant
373 climate responses to subsequent grand solar minima which were also large in amplitude but did not yield an
374 unequivocal impact on North Atlantic climate. It is indeed notable that the following changes in solar activity
375 occurred while the influence of freshwater release by the FIS was diminishing, and therefore the North Atlantic
376 was not conditioned as it was during the PBO. For instance, a similar but weaker event was found in the $\delta^{18}O$
377 signal of the GRIP ice core around 10,300 cal. years BP, coinciding with a low in $\Delta^{14}C$ (high solar activity) and
378 a cooling in the Faroe Islands (Björck et al., 2001). Whereas, the subsequent grand solar minimum which
379 occurred around 9,500 years BP (Vonmoos et al., 2006), at a time during which the FIS had completely vanished
380 (Stroeven et al., 2016), did not coincide with any evident climate oscillation in Greenland.

381

## 5 Conclusions

383 A comparison of new $^{10}Be$ concentration measurements from the varved Meerfelder Maar sediments covering
384 the period 11,310-11,000 years BP to the $^{10}Be$ data from the GRIP ice core in central Greenland showed a
385 combined offset of up to 98 (+33/-21) years between the MFM2012 and GICC05 chronologies. Correcting for
386 this offset allowed us to determine that the 11.4 ka event in Greenland has no coeval counterparts in Meerfelder

Maar and that it coincides with high solar activity. The time-scales synchronization also showed that an environmental shift at MFM starting at 11,250 years BP is coincident with a transition from high solar activity to a particularly long-lasting grand solar minimum as well as with the termination of the 11.4 ka event in Greenland. The termination and onset of these cold oscillations in Greenland and then Meerfelder Maar are thus synchronous with large changes in solar activity which is a pattern reproduced by a number of modeling studies. Finally, we also postulate that a slowdown of the AMOC due to freshwater delivery from, for instance, the Fennoscandian Ice Sheet could have served as a potential amplifier to this signal. The extent of the role that solar activity changes may have played on the climate of Greenland and Europe during the earliest part of the Holocene is unclear. This is due to the different boundary conditions which prevailed at the time compared to today but also to the proxy-evidence from MFM which is difficult to interpret. The main results from this study do however exemplify the usefulness of cosmogenic radionuclides to synchronize different paleo-records in an effort to investigate the timing and spatial distribution of past climate fluctuations with a high chronological precision.

**Author contribution:** FM performed the analysis in correspondence with RM, carried out the sampling with MC and CMP, and did the chemical preparation of the Meerfelder Maar $^{10}$Be samples with help of AA while GP performed the measurements. FM wrote the manuscript. RM, MC, and FM initiated the project. FA provided the Bayesian synchronization and participated in the interpretation of climate reanalysis with JS. SB, AB, MC, and CMP assisted with the interpretation of the proxy data. All authors were involved in editing the manuscript.

**Competing interests:** The authors declare that they have no conflict of interest.

**Acknowledgements**

This work was supported by the Royal Physiographic Society of Lund (grant to FM) and the Swedish Research Council (grant DNR2013-8421 to RM). MC was funded by a grant from the German Research Foundation (DFG grant CZ 227/4-1) and the BaltRap network of the Leibniz Association SAW-2017-IOW2). FA was supported by the Swedish research council (grant DNR2016-00218). ssAA thanks the UAEU for support through the UPAR funding. The authors would like to thank Inger Påhlsson for her help with the chemical preparation of the sediment $^{10}$Be samples for AMS measurements.

**References**

Adolphi, F., and Muscheler, R.: Synchronizing the Greenland ice core and radiocarbon time-scales over the Holocene – Bayesian wiggle-matching of cosmogenic radionuclide records, Clim. Past, 12(1), 15–30, doi:10.5194/cp-12-15-2016, 2016.

Adolphi, F., Muscheler, R., Svensson, A., Aldahan, A., Possnert, G., Beer, J., Sjolte, J., Björck, S., Matthes, K. and Thiéblemont, R.: Persistent link between solar activity and Greenland climate during the Last Glacial Maximum, Nat. Geosci., 7(9), 662–666, doi:10.1038/ngeo2225, 2014.

422  Berggren, A.-M., Aldahan, A., Possnert, G., Haltia-Hovi, E. and Saarinen, T.: 10Be and solar activity cycles in
423      varved lake sediments, AD 1900–2006, J. Paleolimnol., 44(2), 559–569, doi:10.1007/s10933-010-9437-1,
424      2010.

425  Bos, J. A. A., van Geel, B., van der Plicht, J. and Bohncke, S. J. P.: Preboreal climate oscillations in Europe:
426      Wiggle-match dating and synthesis of Dutch high-resolution multi-proxy records, Quat. Sci. Rev., 26(15–
427      16), 1927–1950, doi:10.1016/j.quascirev.2006.09.012, 2007.

428  Björck, S., Kromer, B., Johnsen, S., Bennike, O., Hammarlund, D., Lemdahl, G., Possnert, G., Rasmussen, T. L.,
429      Wohlfarth, B., Hammer, C. U. and Spurk, M.: Synchronized Terrestrial-Atmospheric Deglacial Records
430      Around the North Atlantic, Science, 274(5290), 1155–60, doi:10.1126/SCIENCE.274.5290.1155, 1996.

431  Björck, S., Rundgren, M., Ingólfsson, Ó. and Funder, S.: The Preboreal oscillation around the Nordic Seas:
432      terrestrial and lacustrine responses, J. Quat. Sci., 12(6), 455–465, doi:10.1002/(SICI)1099-
433      1417(199711/12)12:6<455::AID-JQS316>3.0.CO;2-S, 1997.

434  Björck, S., Muscheler, R., Kromer, B., Andresen, C. S., Heinemeier, J., Johnsen, S. J., Conley, D., Koç, N.,
435      Spurk, M. and Veski, S.: High-resolution analyses of an early Holocene climate event may imply
436      decreased solar forcing as an important climate trigger, Geology, 29(12), 1107, doi:10.1130/0091-
437      7613(2001)029<1107:HRAOAE>2.0.CO;2, 2001.

438  Brauer, A., Endres, C., Günter, C., Litt, T., Stebich, M. and Negendank, J. F. W.: High resolution sediment and
439      vegetation responses to Younger Dryas climate change in varved lake sediments from Meerfelder Maar,
440      Germany, Quat. Sci. Rev., 18(3), 321–329, doi:10.1016/S0277-3791(98)00084-5, 1999.

441  Brauer, A., Endres, C., Zolitschka, B. and Negendank, J. F.: AMS radiocarbon and varve chronology from the
442      annually laminated sediment record of Lake Meerfelder Maar, Germany. Radiocarbon, 42(3), 355-368,
443      2000.

444  Bronk Ramsey, C., van der Plicht, J., and Weninger, B.: "Wiggle matching" radiocarbon dates, Radiocarbon, 43,
445      381–390, 2001.

446  Compo, G. P., Whitaker, J. S., Sardeshmukh, P. D., Matsui, N., Allan, R. J., Yin, X., Gleason, B. E., Vose, R. S.,
447      Rutledge, G., Bessemoulin, P., Brönnimann, S., Brunet, M., Crouthamel, R. I., Grant, A. N., Groisman, P.
448      Y., Jones, P. D., Kruk, M. C., Kruger, A. C., Marshall, G. J., Maugeri, M., Mok, H. Y., Nordli, Ø., Ross,
449      T. F., Trigo, R. M., Wang, X. L., Woodruff, S. D. and Worley, S. J.: The Twentieth Century Reanalysis
450      Project, Q. J. R. Meteorol. Soc., 137(654), 1–28, doi:10.1002/qj.776, 2011.

451  Czymzik, M., Adolphi, F., Muscheler, R., Mekhaldi, F., Martin-Puertas, C., Aldahan, A., Oran Possnert, G. €
452      and Brauer, A.: A varved lake sediment record of the 10Be solar activity proxy for the Lateglacial-
453      Holocene transition, Quat. Sci. Rev., 153, 31–39, doi:10.1016/j.quascirev.2016.10.007, 2016.

454  Czymzik, M., Muscheler, R., Adolphi, F., Mekhaldi, F., Dräger, N., Ott, F., Slowinski, M., Blaszkiewicz, M.,
455      Aldahan, A., Possnert, G. and Brauer, A.: Synchronizing 10Be in two varved lake sediment records to
456      IntCal13 14C during three grand solar minima, Clim. Past, 14(5), doi:10.5194/cp-14-687-2018, 2018.

457  Dansgaard, W.: Stable isotopes in precipitation, Tellus, 16(4), 436–468, doi:10.3402/tellusa.v16i4.8993, 1964.

458  Duchez, A., Hirschi, J. J.-M, Cunningham, S. A., Blaker, A. T., Bryden, H. L., De Cuevas, B., Atkinson, C. P.,
459      Mccarthy, G. D., Frajka-Williams, E., Rayner, D., Smeed, D. and Mizielinski, M. S.: A new index for the
460      Atlantic Meridional Overturning Circulation at 26°N., J. of Clim., 27(17), 6439-6455, doi:10.1175/JCLI-
461      D-13-00052.1, 2014.

Dyke, A. S.: An outline of North American deglaciation with emphasis on central and northern Canada, Dev. in Quat. Sci, 2, 373-424, doi.org/10.1016/S1571-0866(04)80209-4, 2004.

Finkel, R. C. and Nishiizumi, K.: Beryllium 10 concentrations in the Greenland Ice Sheet Project 2 ice core from 3-40 ka, J. Geophys. Res. Ocean., 102(C12), 26699–26706, doi:10.1029/97JC01282, 1997.

Fisher, T. G., Smith, D. G. and Andrews, J. T.: Preboreal oscillation caused by a glacial Lake Agassiz flood, Quat. Sci. Rev., 21(8–9), 873–878, doi:10.1016/S0277-3791(01)00148-2, 2002.

Frankignoul, C., Gastineau, G. and Kwon, Y. O.: The influence of the AMOC variability on the atmosphere in CCSM3, J. of Clim., 26(24), 9774-9790, doi.org/10.1175/JCLI-D-12-00862.1, 2013.

Gray, L. J., Scaife, A. A., Mitchell, D. M., Osprey, S., Ineson, S., Hardiman, S., Butchart, N., Knight, J., Sutton, R. and Kodera, K.: A lagged response to the 11 year solar cycle in observed winter Atlantic/European weather patterns, J. Geophys. Res. Atmos., 118(24), 13,405-13,420, doi:10.1002/2013JD020062, 2013.

Haigh, J. D., Winning, A. R., Toumi, R. and Harder, J. W.: An influence of solar spectral variations on radiative forcing of climate, Nature, 467(7316), 696–699, doi:10.1038/nature09426, 2010.

Hald, M. and Hagen, S.: Early Preboreal cooling in the Nordic seas region triggered by meltwater, Geology, doi:10.1130/0091-7613(1998)026<0615:EPCITN>2.3.CO;2, 1998.

Ineson, S., Scaife, A. A., Knight, J. R., Manners, J. C., Dunstone, N. J., Gray, L. J. and Haigh, J. D.: Solar forcing of winter climate variability in the Northern Hemisphere, Nat. Geosci., 4(11), 753–757, doi:10.1038/ngeo1282, 2011.

Kobashi, T., Severinghaus, J. P. and Barnola, J.-M.: 4±1.5 °C abrupt warming 11,270 yr ago identified from trapped air in Greenland ice, Earth Planet. Sci. Lett., 268(3–4), 397–407, doi:10.1016/j.epsl.2008.01.032, 2008.

Kodera, K.: Solar cycle modulation of the North Atlantic Oscillation: Implication in the spatial structure of the NAO, Geophys. Res. Lett., 29(8), 59-1-59–4, doi:10.1029/2001GL014557, 2002.

Lane, C. S., Brauer, A., Martín-Puertas, C., Blockley, S. P. E., Smith, V. C. and Tomlinson, E. L.: The Late Quaternary tephrostratigraphy of annually laminated sediments from Meerfelder Maar, Germany, Quat. Sci. Rev., 122, 192-206, doi:10.1016/j.quascirev.2015.05.025, 2015.

Lockwood, M., Bell, C., Woollings, T., Harrison, R. G., Gray, L. J. and Haigh, J. D.: Top-down solar modulation of climate: evidence for centennial-scale change, Environ. Res. Lett., 5(3), 34008, doi:10.1088/1748-9326/5/3/034008, 2010.

Löfverström, M. and Lora, J. M.: Abrupt regime shifts in the North Atlantic atmospheric circulation over the last deglaciation, Geophys. Res. Lett., 44(15), 8047–8055, doi:10.1002/2017GL074274, 2017.

Magny, M., Vannière, B., de Beaulieu, J.-L., Bégeot, C., Heiri, O., Millet, L., Peyron, O. and Walter-Simonnet, A.-V.: Early-Holocene climatic oscillations recorded by lake-level fluctuations in west-central Europe and in central Italy, Quat. Sci. Rev., 26(15–16), 1951–1964, doi:10.1016/j.quascirev.2006.04.013, 2007.

Martin-Puertas, C., Brauer, A., Dulski, P. and Brademann, B.: Testing climate–proxy stationarity throughout the Holocene: an example from the varved sediments of Lake Meerfelder Maar (Germany), Quat. Sci. Rev., 58, 56–65, doi:10.1016/J.QUASCIREV.2012.10.023, 2012a.

Martin-Puertas, C., Matthes, K., Brauer, A., Muscheler, R., Hansen, F., Petrick, C., Aldahan, A., Possnert, G. and van Geel, B.: Regional atmospheric circulation shifts induced by a grand solar minimum, Nat. Geosci., 5(6), 397–401, doi:10.1038/ngeo1460, 2012b.

502 Martin-Puertas, C., Tjallingii, R., Bloemsma, M. and Brauer, A.: Varved sediment responses to early Holocene
503      climate and environmental changes in Lake Meerfelder Maar (Germany) obtained from multivariate
504      analyses of micro X-ray fluorescence core scanning data, J. Quat. Sci., 32(3), 427–436,
505      doi:10.1002/jqs.2935, 2017.

506 Masson-Delmotte, V., Landais, A., Stievenard, M., Cattani, O., Falourd, S., Jouzel, J., Johnsen, S. J., Dahl-
507      Jensen, D., Sveinsbjornsdottir, A., White, J. W. C., Popp, T. and Fischer, H.: Holocene climatic changes in
508      Greenland: Different deuterium excess signals at Greenland Ice Core Project (GRIP) and NorthGRIP, J.
509      Geophys. Res. Atmos., 110(D14), n/a-n/a, doi:10.1029/2004JD005575, 2005.

510 Matthes, K., Kuroda, Y., Kodera, K. and Langematz, U.: Transfer of the solar signal from the stratosphere to the
511      troposphere: Northern winter, J. Geophys. Res., 111(D6), D06108, doi:10.1029/2005JD006283, 2006.

512 McCarthy, G. D., Haigh, I. D., Hirschi, J. J. M., Grist, J. P., and Smeed, D. A.: Ocean impact on decadal Atlantic
513      climate variability revealed by sea-level observations, Nature, 521(7553), 508, doi:10.1038/nature14491,
514      2015.

515 Merz, N., Raible, C. C. and Woollings, T.: North Atlantic Eddy-Driven Jet in Interglacial and Glacial Winter
516      Climates, J. Clim., 28(10), 3977–3997, doi:10.1175/JCLI-D-14-00525.1, 2015.

517 Moffa-Sánchez, P., Born, A., Hall, I. R., Thornalley, D. J. R. and Barker, S.: Solar forcing of North Atlantic
518      surface temperature and salinity over the past millennium, Nat. Geosci., 7(4), 275–278,
519      doi:10.1038/ngeo2094, 2014.

520 Muscheler, R., Beer, J., Wagner, G., Laj, C., Kissel, C., Raisbeck, G. M., Yiou, F. and Kubik, P. W.: Changes in
521      the carbon cycle during the last deglaciation as indicated by the comparison of 10Be and 14C records,
522      Earth Planet. Sci. Lett., 219(3–4), 325–340, doi:10.1016/S0012-821X(03)00722-2, 2004.

523 Muscheler, R., Kromer, B., Björck, S., Svensson, A., Friedrich, M., Kaiser, K. F. and Southon, J.: Tree rings and
524      ice cores reveal 14C calibration uncertainties during the Younger Dryas, Nat. Geosci., 1(4), 263–267,
525      doi:10.1038/ngeo128, 2008.

526 Muscheler, R., Adolphi, F. and Knudsen, M. F.: Assessing the differences between the IntCal and Greenland ice-
527      core time scales for the last 14,000 years via the common cosmogenic radionuclide variations, Quat. Sci.
528      Rev., 106, 81–87, doi:10.1016/J.QUASCIREV.2014.08.017, 2014.

529 Ortega, P., Lehner, F., Swingedouw, D., Masson-Delmotte, V., Raible, C. C., Casado, M. and Yiou, P.: A
530      model-tested North Atlantic Oscillation reconstruction for the past millennium, Nature, 523(7558), 71–74,
531      doi:10.1038/nature14518, 2015.

532 Pedro, J. B., Mcconnell, J. R., Van Ommen, T. D., Fink, D., Curran, M. A. J., Smith, A. M., Simon, K. J., Moy,
533      A. D. and Das, S. B.: Solar and climate influences on ice core 10 Be records from Antarctica and
534      Greenland during the neutron monitor era, Aust. Nucl. Sci. Technol. Organ.,
535      doi:10.1016/j.epsl.2012.08.038, 2012.

536 Rach, O., Brauer, a., Wilkes, H. and Sachse, D.: Delayed hydrological response to Greenland cooling at the
537      onset of the Younger Dryas in western Europe, Nat. Geosci., 7(2), 109–112, doi:10.1038/ngeo2053, 2014.

538 Rasmussen, S. O., Andersen, K. K., Svensson, A. M., Steffensen, J. P., Vinther, B. M., Clausen, H. B., Siggaard-
539      Andersen, M.-L., Johnsen, S. J., Larsen, L. B., Dahl-Jensen, D., Bigler, M., Röthlisberger, R., Fischer, H.,
540      Goto-Azuma, K., Hansson, M. E. and Ruth, U.: A new Greenland ice core chronology for the last glacial
541      termination, J. Geophys. Res., 111(D6), D06102, doi:10.1029/2005JD006079, 2006.

542 Rasmussen, S. O., Vinther, B. M., Clausen, H. B. and Andersen, K. K.: Early Holocene climate oscillations
543      recorded in three Greenland ice cores, Quat. Sci. Rev., 26(15–16), 1907–1914,
544      doi:10.1016/j.quascirev.2007.06.015, 2007.

545 Rasmussen, S. O., Bigler, M., Blockley, S. P., Blunier, T., Buchardt, S. L., Clausen, H. B., Cvijanovic, I., Dahl-
546      Jensen, D., Johnsen, S. J., Fischer, H., Gkinis, V., Guillevic, M., Hoek, W. Z., Lowe, J. J., Pedro, J. B.,
547      Popp, T., Seierstad, I. K., Steffensen, J. P., Svensson, A. M., Vallelonga, P., Vinther, B. M., Walker, M. J.
548      C., Wheatley, J. J. and Winstrup, M.: A stratigraphic framework for abrupt climatic changes during the
549      Last Glacial period based on three synchronized Greenland ice-core records: refining and extending the
550      INTIMATE event stratigraphy, Quat. Sci. Rev., 106, 14–28, doi:10.1016/J.QUASCIREV.2014.09.007,
551      2014.

552 Reimer, P. J., Bard, E., Bayliss, A., Beck, J. W., Blackwell, P. G., Ramsey, C. B., Buck, C. E., Cheng, H.,
553      Edwards, R. L., Friedrich, M., Grootes, P. M., Guilderson, T. P., Haflidason, H., Hajdas, I., Hatté, C.,
554      Heaton, T. J., Hoffmann, D. L., Hogg, A. G., Hughen, K. A., Kaiser, K. F., Kromer, B., Manning, S. W.,
555      Niu, M., Reimer, R. W., Richards, D. A., Scott, E. M., Southon, J. R., Staff, R. A., Turney, C. S. M. and
556      van der Plicht, J.: IntCal13 and Marine13 Radiocarbon Age Calibration Curves 0–50,000 Years cal BP,
557      Radiocarbon, 55(4), 1869–1887, doi:10.2458/azu_js_rc.55.16947, 2013.

558 Seierstad, I. K., Abbott, P. M., Bigler, M., Blunier, T., Bourne, A. J., Brook, E., Buchardt, S. L., Buizert, C.,
559      Clausen, H. B., Cook, E., Dahl-Jensen, D., Davies, S. M., Guillevic, M., Johnsen, S. J., Pedersen, D. S.,
560      Popp, T. J., Rasmussen, S. O., Severinghaus, J. P., Svensson, A. and Vinther, B. M.: Consistently dated
561      records from the Greenland GRIP, GISP2 and NGRIP ice cores for the past 104 ka reveal regional
562      millennial-scale δ18O gradients with possible Heinrich event imprint, Quat. Sci. Rev., 106, 29–46,
563      doi:10.1016/J.QUASCIREV.2014.10.032, 2014.

564 Simpson, I. R., Blackburn, M., Haigh, J. D., Simpson, I. R., Blackburn, M. and Haigh, J. D.: The Role of Eddies
565      in Driving the Tropospheric Response to Stratospheric Heating Perturbations, J. Atmos. Sci., 66(5), 1347–
566      1365, doi:10.1175/2008JAS2758.1, 2009.

567 Sjolte, J., Sturm, C., Adolphi, F., Vinther, B. M., Werner, M., Lohmann, G. and Muscheler, R.: Solar and
568      volcanic forcing of North Atlantic climate inferred from a process-based reconstruction, Clim. Past, 14,
569      1179–1194, doi:10.5194/cp-14-1179-2018, 2018.

570 Southon, J.: A First Step to Reconciling the GRIP and GISP2 Ice-Core Chronologies, 0–14,500 yr B.P., Quat.
571      Res., 57(1), 32–37, doi:10.1006/qres.2001.2295, 2002.

572 Steig, E.J., Grootes, P.M. and Stuiver, M.: Seasonal Precipitation Timing and Ice Core Records. Science, 266,
573      1885–1886, doi.org/10.1126/science.266.5192.1885, 1994.

574 Stroeven, A. P., Hättestrand, C., Kleman, J., Heyman, J., Fabel, D., Fredin, O., Goodfellow, B. W., Harbor, J.
575      M., Jansen, J. D., Olsen, L., Caffee, M. W., Fink, D., Lundqvist, J., Rosqvist, G. C., Strömberg, B. and
576      Jansson, K. N.: Deglaciation of Fennoscandia, Quat. Sci. Rev., 147, 91–121,
577      doi:10.1016/J.QUASCIREV.2015.09.016, 2016.

578 Stuiver, M. and Polach, H. A.: Discussion Reporting of 14C Data, Radiocarbon, 19(3), 355–363,
579      doi:10.1017/S0033822200003672, 1977.

580 Svalgaard, L. and Schatten, K. H.: Reconstruction of the Sunspot Group Number: The Backbone Method, Sol.
581      Phys., 291(9–10), 2653–2684, doi:10.1007/s11207-015-0815-8, 2016.

Svensson, A., Andersen, K. K., Bigler, M., Clausen, H. B., Dahl-Jensen, D., Davies, S. M., Johnsen, S. J., Muscheler, R., Parrenin, F., Rasmussen, S. O., Röthlisberger, R., Seierstad, I., Steffensen, J. P. and Vinther, B. M.: A 60 000 year Greenland stratigraphic ice core chronology, Clim. Past, 4, 47–57, doi.org/10.5194/cp-4-47-2008, 2008.

van der Plicht, J., van Geel, B., Bohncke, S. J. P., Bos, J. A. A., Blaauw, M., Speranza, A. O. M., Muscheler, R. and Björck, S.: The Preboreal climate reversal and a subsequent solar-forced climate shift, J. Quat. Sci., 19(3), 263–269, doi:10.1002/jqs.835, 2004.

Vinther, B. M., Clausen, H. B., Johnsen, S. J., Rasmussen, S. O., Andersen, K. K., Buchardt, S. L., Dahl-Jensen, D., Seierstad, I. K., Siggaard-Andersen, M.-L., Steffensen, J. P., Svensson, A., Olsen, J. and Heinemeier, J.: A synchronized dating of three Greenland ice cores throughout the Holocene, J. Geophys. Res., 111(D13), D13102, doi:10.1029/2005JD006921, 2006.

Vinther, B. M., Buchardt, S. L., Clausen, H. B., Dahl-Jensen, D., Johnsen, S. J., Fisher, D. A., Koerner, R. M., Raynaud, D., Lipenkov, V., Andersen, K. K., Blunier, T., Rasmussen, S. O., Steffensen, J. P. and Svensson, A. M.: Holocene thinning of the Greenland ice sheet, Nature, 461(7262), 385–388, doi:10.1038/nature08355, 2009.

von Grafenstein U., Erlenkeuser, H., Brauer, A., Jouzel, J. and Johnsen, S. J.: A mid-european decadal isotope-climate record from 15,500 to 5000 years B.P, Science, 284(5420), 1654–7, doi:10.1126/SCIENCE.284.5420.1654, 1999.

Vonmoos, M., Beer, J. and Muscheler, R.: Large variations in Holocene solar activity: Constraints from 10 Be in the Greenland Ice Core Project ice core, J. Geophys. Res., 111(A10), A10105, doi:10.1029/2005JA011500, 2006.

White, J. W. C., Barlow, L. K., Fisher, D., Grootes, P. M., Jouzel, J., Johnsen, S. J., Stuiver, M. and Clausen, H.B.: Stable isotope stacks from GRIP and GISP ice cores, https://doi.org/10.1594/PANGAEA.716878, 2009.

Woollings, T., Lockwood, M., Masato, G., Bell, C. and Gray, L.: Enhanced signature of solar variability in Eurasian winter climate, Geophys. Res. Lett., 37(20) doi:10.1029/2010GL044601, 2010.
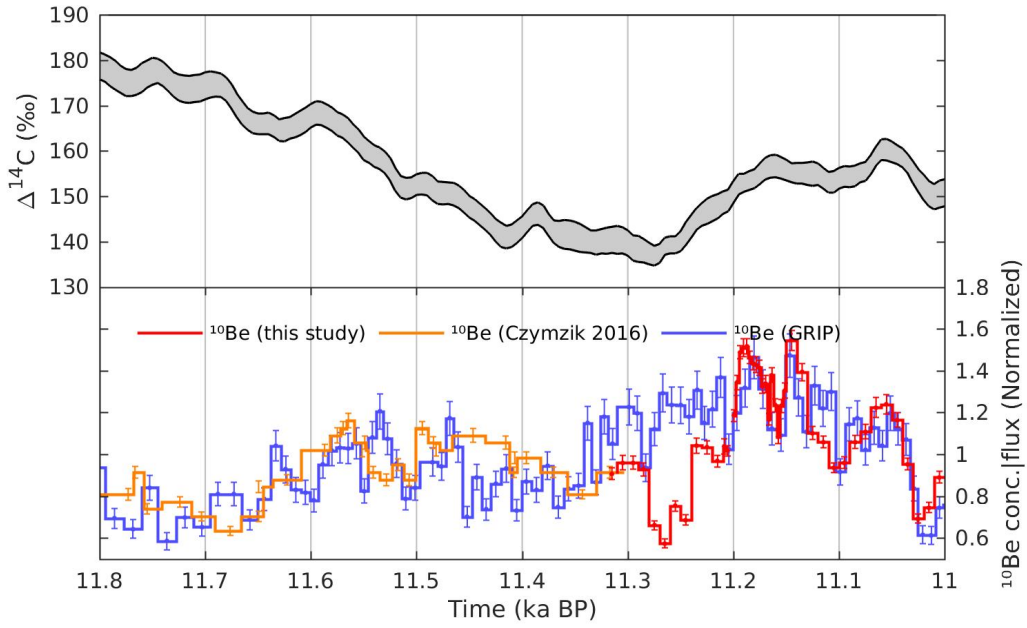
**Figure 1:** Upper panel: The IntCal13 calibration curve (Reimer et al., 2013) expressed as $\Delta^{14}$C (see text). Bottom panel: The $^{10}$Be concentration data from Meerfelder maar (MFM), spanning the period 11,310-11,000 years BP are plotted in red with corresponding measurement error bars. The record is completed in orange with the $^{10}$Be measurements from the same sediment profile for the Late Glacial-Holocene transition (Czymzik et al., 2016). The MFM $^{10}$Be data are plotted on the original MFM2012 chronology. The $^{10}$Be flux data from the GRIP ice core in central Greenland (Adolphi et al., 2014) is plotted in blue and on the GICC05 time-scale (Rasmussen et al., 2006; Vinther et al., 2006; Svensson et al., 2008; Seierstad et al., 2014). All records have been normalized to their mean.
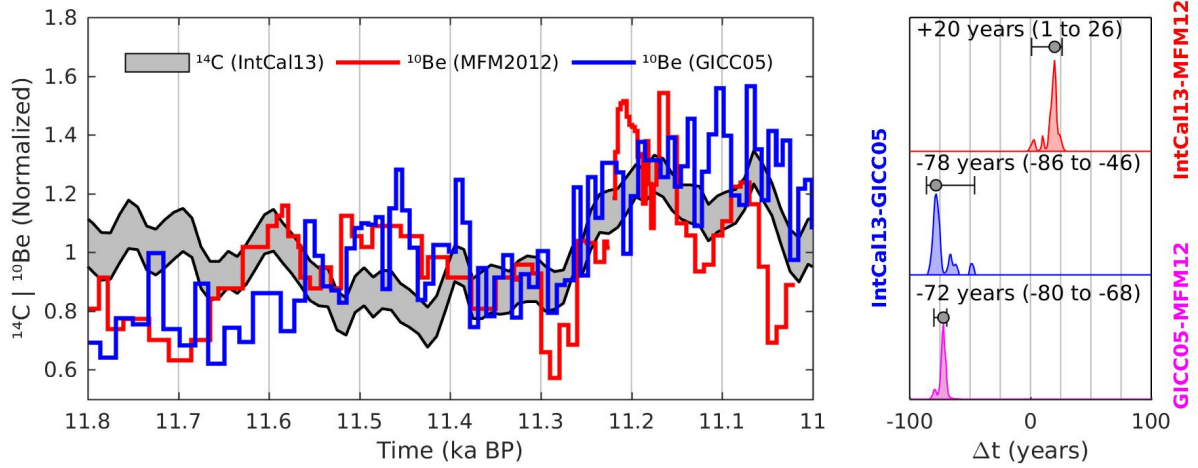
650
651 Figure 2: Results from the Bayesian wiggle-matching of the different radionuclide records. The left panel shows both the
652 MFM [10]Be data (in red) and the GRIP [10]Be data (blue) once synchronized to the ^{14}C production rate data inferred from the
653 IntCal13 calibration curve (1σ grey envelope). The right-hand panel displays the probability density functions for the best
654 fit between IntCal13-MFM2012 (in red), IntCal13-GICC05 (in blue) and GICC05-MFM2012 (in magenta), which resulted in
655 the synchronization in the left-hand panel and with a 95.4% confidence interval illustrated by the horizontal error bars.

656

657
658
659
660
661
662
663
664
665
666
667
668
669
670
671
672
673
674
675
676
677
678
679
680
681
682
683
684
685
686
687
688
689
690
691
692
693
694
695
696
697
698
699
700
701
702
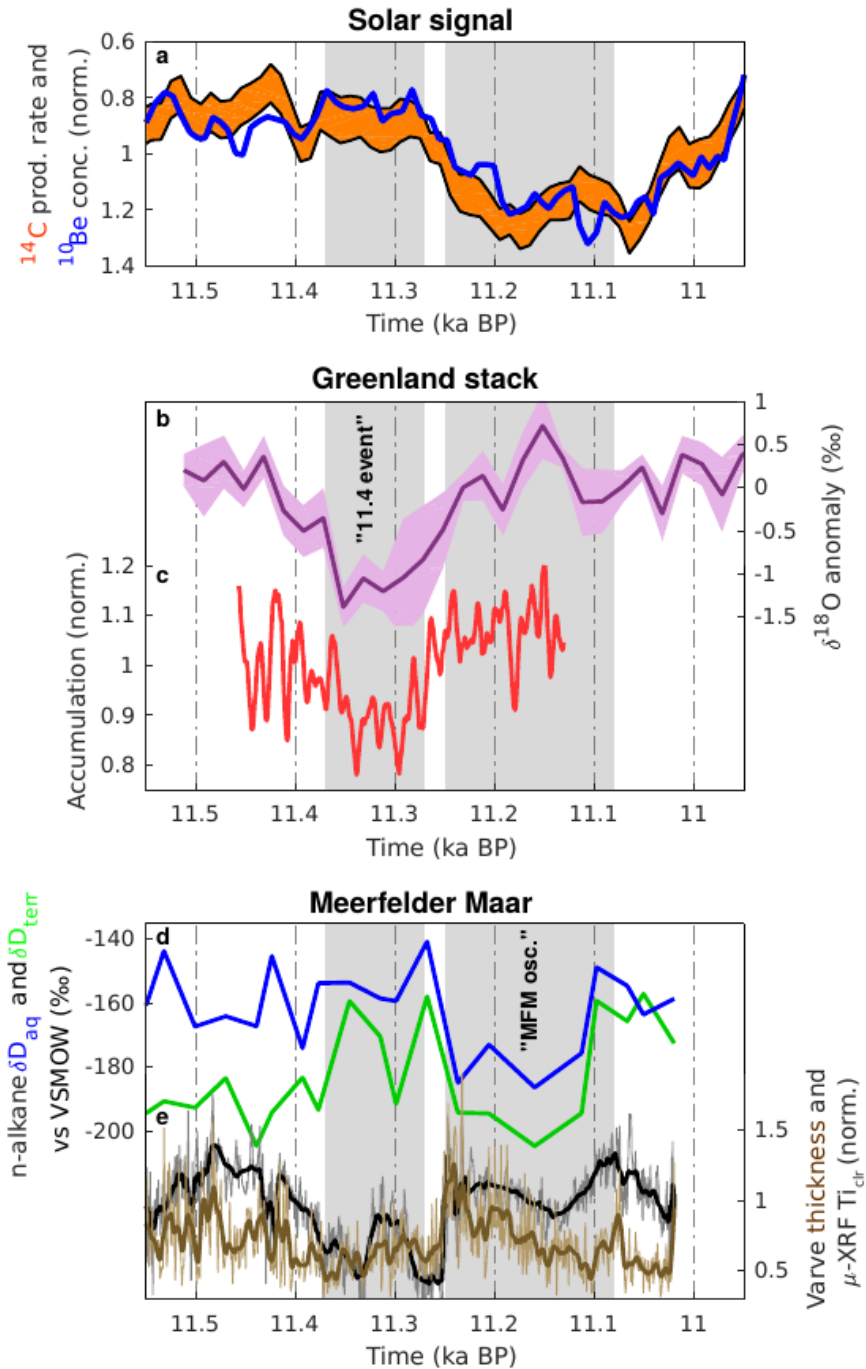
**Figure 3:** (a) ¹⁴C production rate (orange envelope) and GRIP ¹⁰Be data (blue) on a reversed y-axis to indicate variations in solar activity. (b) The δ¹⁸O stack from the DYE-3, GRIP, NGRIP and Renland ice cores (Rasmussen et al., 2007; Vinther et al., 2009) is shown in magenta and (c) the modeled accumulation anomalies from Rasmussen et al. (2007) for DYE-3, GRIP, and NGRIP are shown in red. (d) The δD data record from lipid biomarkers of MFM sediments (Rach et al., 2014) is plotted in blue and green (aquatic and terrestrial) while (e) varve thickness (Martin-Puertas et al., 2012a) and varve μ-XRF Ti$_{clr}$ (Martin-Puertas et al., 2017) are plotted in brown and black, respectively. The grey bands depict the time of occurrence of the 11.4 ka event in Greenland and of the cold oscillation inferred from the MFM sediments (MFM oscillation). All data are plotted on the IntCal13 time-scale, as per Fig. 2.
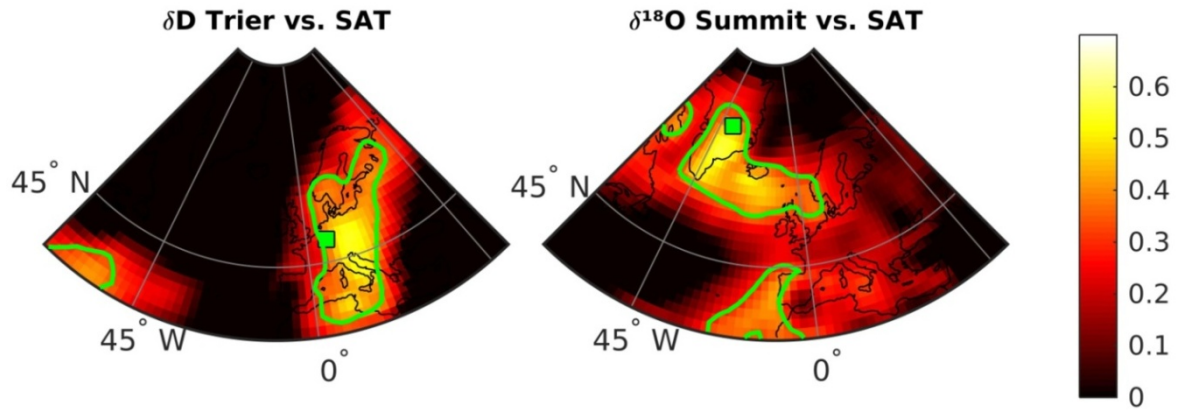
**Figure 4: Left - Correlation map between annual δD in precipitation from the Trier station (green square – IAEA/WMO, 2016) and annual surface air temperatures in the NOAA-CIRES 20th climate reanalysis V2c (Compo et al., 2011) for the period AD 1978-2011. Right – Same as the left panel but for δ18O from the GISP2 ice core (green square – Steig et al., 1994; White et al., 2009) and for the period AD 1950-1986. Green contour lines represent significance levels for p < 0.1 (t-test). The difference in years selected arises from the different time-span of the δD and δ18O records used here.**
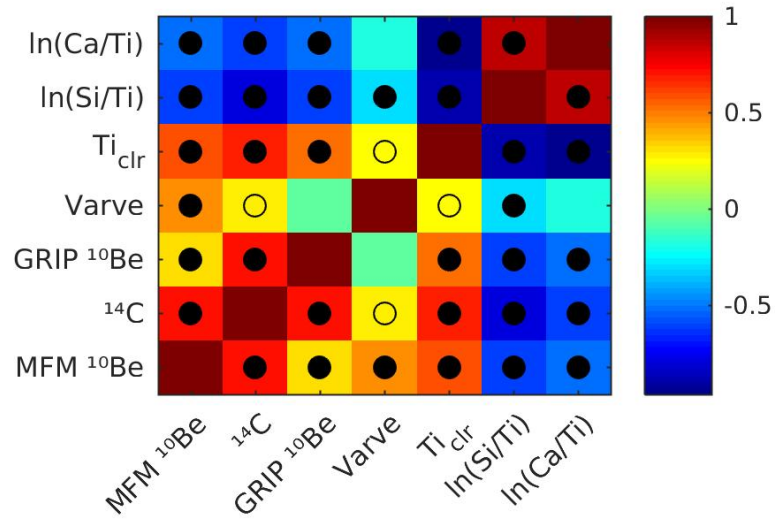
**Figure 5: Color-coded correlation matrix between MFM $^{10}$Be concentration, GRIP $^{10}$Be flux, $^{14}$C production rate data, varve thickness, and μ-XRF data from MFM09 (Martin-Puertas et al., 2017). Open and filled circles denote significant correlations to the p <0.1 and the p <0.05 levels, respectively. All data were binned after the resolution of the MFM $^{10}$Be concentration data for the period 11,310-11,000 years BP and a student t-test was performed to test the significance levels.**
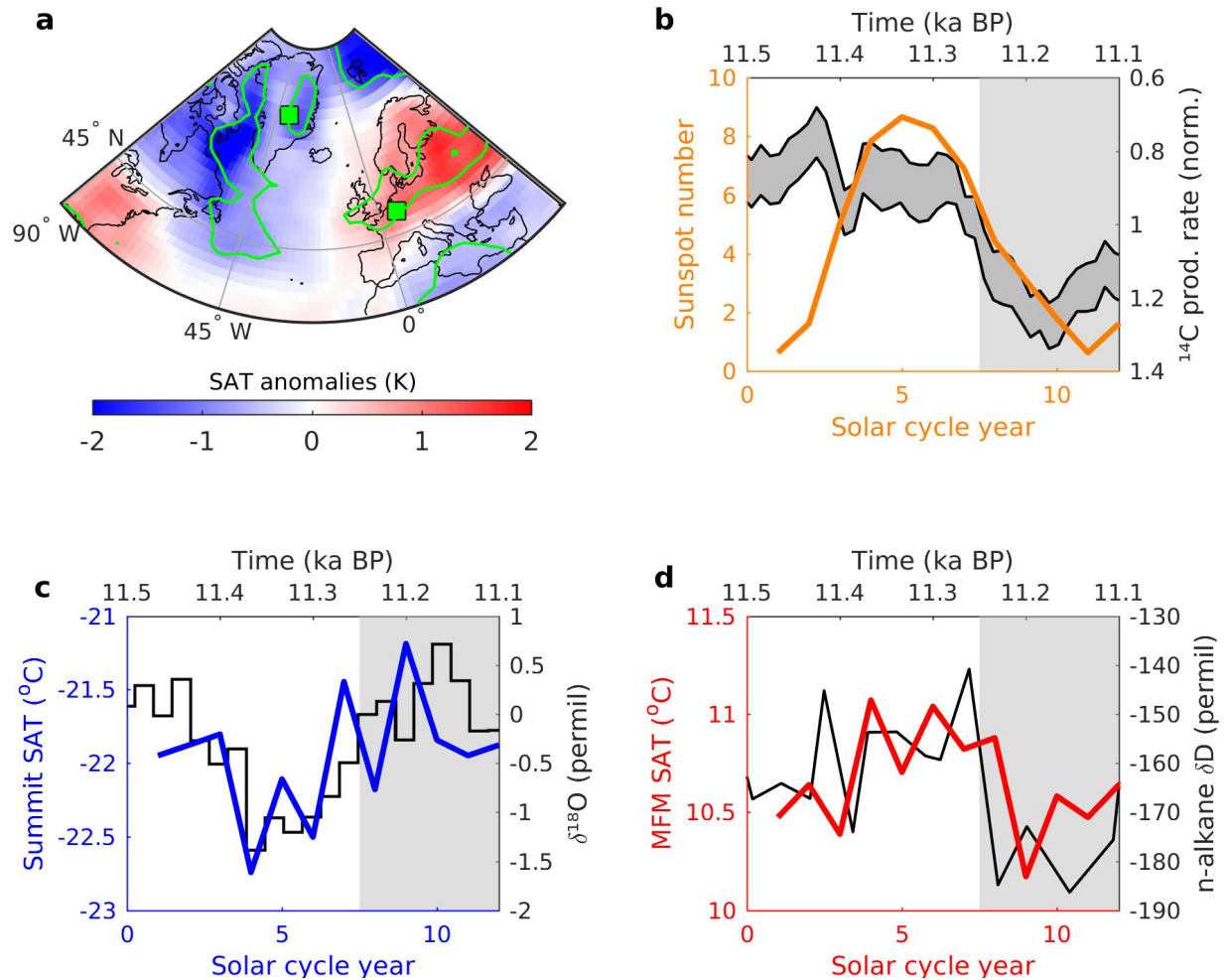
Figure 6: The 11.4 ka event and MFM oscillation compared to solar forcing of 20th century SAT in the North Atlantic region, as seen in 20CR. (a) Surface air temperature (SAT) anomalies for solar maxima winters (DJF) compared to solar minima winters (see Sup. Fig. 2) for the period 1946-2011 in 20th century climate reanalysis (Compo et al., 2011). The green squares point to the location of Summit and of MFM while the green contour lines represent significance levels for p < 0.1 (t-test). Years influenced by large tropical volcanic eruptions have been removed, as per Ineson et al. (2011). (b) The transition between high to low solar activity in the $^{14}$C production rate data (grey envelope - top and right axes) compared to the mean sunspot group number of all 11-year solar cycles during 1900-2011 (orange curve - bottom and left axes). (c) The δ18O stack (black curve - top and right axes) shown in Fig. 3b compared to the mean SAT at Summit (blue curve; bottom and left axes) throughout all 11-year solar cycles between 1900-2011 as in (b). (d) Same as (c) but with δD (black curve – top and right axes) and MFM SAT (red curve – bottom and left axes). Note the different time scale on the top (paleo records) and bottom axes (reanalysis data). The grey bands show the periods of low solar activity occurring on the two time periods that are compared.

738
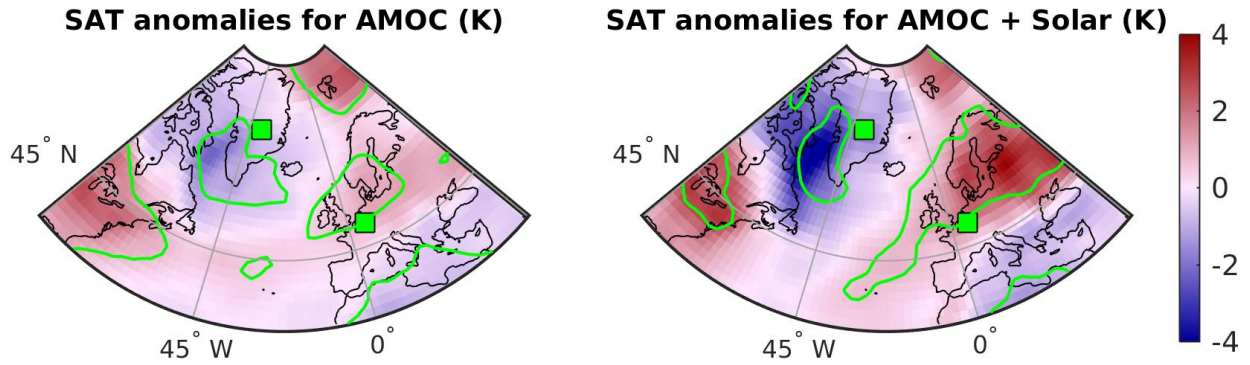
739
740
741 **Figure 7: Left - Winter (DJF) surface air temperature anomalies for negative AMOC years compared to positive AMOC**
742 **years for the period 1961-2005 in 20th century climate reanalysis (see Sup. Fig. 4). The green markers point to the**
743 **location of Summit and of MFM while the green contour lines represent significance levels for p < 0.1 (t-test). Right -**
744 **Same as left panel but for years of both negative AMOC and high solar activity.**

745
746
747
748
749
750
751
752
753
754
755
756
757
758
759
760
761
762
763
764
765
766
767
768
769
770
771
772
773
774
775
776